Energy Proceedings
2022
ISSN 2004-2965

Comparison of different control strategies for PEM fuel cells thermal management system for Zero Emission Ship (ZEUS) onboard power generation.

Cavo M[1], Rivarolo M[1], Gini L[1], Gadducci E[1], Massardo AF[1]

1 Thermochemical Power Group, DIME, Università degli Studi di Genova

ABSTRACT

The present paper aims to analyse the thermal coupling of PEM fuel cells fed by hydrogen, stored in metal hydride tanks for maritime applications, considering the first Italian zero emissions ship with hydrogen PEM fuel cells propulsion (ZEUS), launched in 2022. A dynamic model is developed, and the integrated propulsion system is analysed in different operative conditions, considering the transitory that can be experimented during navigation (i.e., from harbour to cruise speed). The behaviour of the fuel cells in dynamic conditions is investigated, considering two different control systems, based on PID and Model Predictive Control approaches.

Keywords: advanced energy technologies, control strategy, energy systems, fuel cells, hydrogen storage.

NOMENCLATURE

Abbreviations	
DMPC	Discrete Model Predictive Control
FCS	Fuel Cell System
IMO	International Maritime Organization
MH	Metal Hydride
MPC	Model Predictive Controller
PEM	Proton Exchange Membrane
PID	Proportional Integrative Derivative
WGHE	Water Glycol Heat Exchanger
ZEUS	Zero Emission Ultimate Ship
Symbols	
e	Error between set-point and measure
J	MPC Cost Function
k	Continuous time
K_D	PID derivative coefficient
K_I	PID integral coefficient
K_P	PID proportional coefficient
R	MPC control weight matrix
Q	MPC state weight matrix
u	Control signal
t	Continuous time
x	State vector of NMSS
y	Output of NMSS

1. INTRODUCTION

As CO_2 anthropogenic emissions are dramatically increasing [1], the importance of new energy policies to reduce their impact is internationally recognized. Maritime transportation sector has a significant impact, with a recent increase from 962 Mt in 2012 to 1056 Mt in 2018 [2]. In recent years, International Maritime Organization (IMO) set long-term targets to reduce 50% GHG emissions by 2050, compared to 2008 levels [3]. To reach this target, different strategies are possible, such as (i) using low-impact fuels as ammonia, methanol or hydrogen [4][5][6][7]; (ii) increase energy efficiency onboard [8]; (iii) designing vessels with lower resistance [9].

The installation of Fuel Cell Systems (FCS) onboard can represent a worthy solution for maritime applications [10][11][12][13][14], as they have high efficiency, low noise/vibrations, and low pollutant emissions. Recent literature reports many possible fuel cells' use in maritime field as an alternative to traditional engines fed by diesel, up to 1 MW size [15][16][17]. Proton Exchange Membrane (PEM) Fuel Cells, fed by pure H_2, represent the most promising technology, thanks to their compactness, fast answer to load variations and zero impact in terms of emissions. These features recently encouraged researchers to investigate solutions for PEM Fuel Cells and hybrid systems modelling [18][19][20][21][22], also considering dynamic conditions [23][24].

A key-point related to PEM Fuel Cells application for sustainable mobility is related to H_2 storage, considering the limitations for high-pressure and liquid H_2 tanks, as significant volumes are needed onboard [25]. Metal Hydrides (MH) are an interesting alternative solution, as they are characterized by high volumetric energy density, as reported in [26][27]; their main drawback is related to the considerable weight, but this aspect can be overcome for maritime applications by properly installing the MH tanks onboard ships. The thermal coupling of FCS and MH has been recently investigated by many researchers: as H_2 desorption from MH tanks is

This is a paper for the 14th International Conference on Applied Energy - ICAE2022, Aug. 8-11, 2022, Bochum, Germany.

an endothermal reaction, the needed heat input can be recovered from the FCS [28][29][30].

In previous research, the authors developed a control system for the FCS-MH system management throughout a model-based approach and tested the dynamic behavior in several conditions [29]. However, a proper control is mandatory to answer to fast load variations, to avoid stressing PEM Fuel Cells, which represent the propulsion system onboard, integrated with electrical batteries.

The aim of this paper is to test the thermal management loop of the FCS+MH propulsion system for maritime applications. A dynamic model in MATLAB-Simulink has been developed and validated for this scope and two different control strategies are compared considering a typical operative load profile.

2. MODEL DESCRIPTION

The thermal management system of the PEM Fuel Cells and MH energy production plant is modelled in the MATLAB-Simulink environment. This section describes the adopted approach and the assumptions to develop the model. The PID and the MPC methods are applied to the same system control strategy and compared.

The system modelled in this work consists of two power generation branches based on PEMFC technology (Figure 1), installed power 71 kW for each branch. The heat produced by the stacks is dissipated through two heat exchangers: WGHE-1 and 2. They are crossed by the cooling fluid of the PEM modules (water and glycol mixture) and the heating fluid of the metal hydrides (water). The heat produced by the stacks feeds the hydrogen release reactions in the MH. The excess heat energy is dissipated through a water sea heat exchanger (WSHE): the cold source is seawater at 15°C. Each heat exchanger may be bypassed by 3-way valves: the control system manages the opening of these valves to keep the system in ideal operating condition.

2.1 Thermal management system model

A model in the MATLAB-Simulink environment has been developed to represent the dynamic interaction between the control systems and the main components constituting the thermal management system of metal hydrides and FCS. The constitutive equations of the main components are summarized in Table 1. More details are provided in [29]. Each model has been validated according to data provided by the manufacturer.

The PID control system allows the minimization of the error against the setpoint through the three constituent contributions as shown in (1).

$$u(t) = K_P e(t) + K_I \int e(\tau) d\tau + K_D \frac{d\, e(t)}{dt} \qquad (1)$$

Each characteristic constant (K_P, K_I, K_D) has been characterized following a trial-and-error process.

The MPC model is based on a function for Discrete Model Predictive Control (DMPC) and one for the observer, according to the velocity form presented by Wang and Young [31]. An augmented representation of the state space (NMSS), as reported in [31][32], was used for the development of the control model: the state of the system at each time step, which must be reported to the dynamic DMPC model, is calculated by the observer (2).

$$\begin{vmatrix}\Delta \boldsymbol{x_m}(\boldsymbol{k}+\boldsymbol{1})\\ \boldsymbol{y}(\boldsymbol{k}+\boldsymbol{1})\end{vmatrix} = \begin{vmatrix}\boldsymbol{A_m} & \boldsymbol{0_p^T}\\ \boldsymbol{C_m A_m} & \boldsymbol{1}\end{vmatrix}\begin{vmatrix}\Delta \boldsymbol{x_m}(\boldsymbol{k})\\ \boldsymbol{y}(\boldsymbol{k})\end{vmatrix} + \begin{vmatrix}\boldsymbol{B_m}\\ \boldsymbol{C_m B_m}\end{vmatrix}\Delta \boldsymbol{u}(\boldsymbol{k})$$
$$\boldsymbol{y}(\boldsymbol{k}) = |\boldsymbol{0_m} \quad \boldsymbol{1}| \begin{vmatrix}\Delta \boldsymbol{x_m}(\boldsymbol{k})\\ \boldsymbol{y}(\boldsymbol{k})\end{vmatrix} \qquad (2)$$

Laguerre's network is used to perform an excellent approximation of the original transfer function model within the MPC. Control tuning is based on the DLQR architecture, minimizing cost function *J*, where *Q* and *R* are the weight matrices, *x* is the state of NMSS and *u* is the control signal (3). This algorithm includes constraints on the rate of increase of the output variable.

$$J = \frac{1}{2} x^T Q x + u^T R u \qquad (3)$$

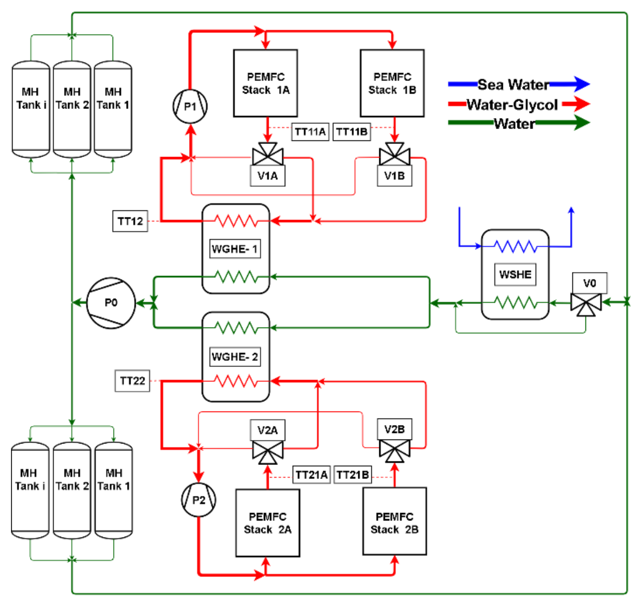

Fig. 1: PEMFC and MH thermal management system layout.

Table 1: description of model main equations. For more details [29]

PEM Fuel Cell model
$V_{cell} = 1.229 - 0.85\ 10^{-3}(T_{st} - 298.15) + \frac{R}{2\,F} T_{st} \left[\ln(p_{H_2}) + \frac{1}{2}\ln(p_{O_2})\right] - V_{act} - V_{ohm}$
$Q_{ST} = (V_{act} + V_{ohm})\, i\, n$

$$P_{el} = (i\, V_{cell})n$$
$$Q_{exch} = Q_{max}\, \varepsilon$$
$$\frac{dT_{out,COOL}}{dt} = \frac{1}{M_{COOL}\, c_{p_{COOL}}}\left(\dot{m}_{COOL} c_{p_{COOL}}\left(T_{in,COOL} - T_{out,COOL}\right) + Q_{exch}\right)$$
$$\dot{m}_{H_2,stech} = n\frac{i}{2\,F} MM_{H_2}$$
$$P_{el,NET} = P_{el}\, \eta_{DC/DC} - BoP$$

MH model

$$\left(\frac{v_{tank}}{v_{MH}} - 1 + e\right)\frac{d\rho_g}{dt} = -n_d - \frac{\dot{m}_{H_2,out}}{v_{MH}}$$
$$n_d = C_d exp\left(\frac{-E_d}{RT_{MH}}\right)\left(\frac{p_g - p_{eq}}{p_{eq}}\right)(\rho_s - \rho_0)$$
$$\nu_{MH}\left(e\rho_g c_{p_g} + (1-e)\rho_s c_{p_s}\right)\frac{\partial T_{MH}}{\partial t} = K_e \nabla^2 T_{MH} + Q + S_{TH}$$

WGHE and WSHE models

$$Q_{exch,COLD,j} = U_{COLD}\frac{A_{COLD}}{N}\left(T_{METAL,j} - T_{COLD,j}\right)$$
$$Q_{exch,HOT,j} = U_{HOT}\frac{A_{HOT}}{N}\left(T_{HOT,j} - T_{METAL,j}\right)$$
$$Q_{exch,HOT,j} = U_{HOT}\frac{A_{HOT}}{N}\left(T_{HOT,j} - T_{METAL,j}\right)$$
$$Q_{exch,METAL,j} = k\frac{N}{L}A_{METAL}\left(T_{METAL,j-1} - T_{METAL,j}\right) + k\frac{N}{L}A_{METAL}\left(T_{METAL,j+1} - T_{METAL,j}\right)$$
$$\frac{dT_{HOT,j}}{dt} = \frac{N}{M_{HOT}\, c_{p_{HOT}}}\left(\dot{m}_{HOT} c_{p_{HOT}}\left(T_{in,HOT,j} - T_{HOT,j}\right) - Q_{exch,HOT,j}\right)$$
$$\frac{dT_{COLD,j}}{dt} = \frac{N}{M_{COLD}\, c_{p_{COLD}}}\left(\dot{m}_{COLD} c_{p_{COLD}}\left(T_{in,COLD,j} - T_{COLD,j}\right) + Q_{exch,COLD,j}\right)$$
$$\frac{dT_{METAL,j}}{dt} = \frac{N}{M_{METAL} c_{p_{METAL}}}\left(Q_{exch,METAL,j} + Q_{exch,HOT,j} - Q_{exch,COLD,j}\right)$$

Pump model

$$\dot{Q} = \frac{H_0}{H_{nominal}k} - \left(\frac{H}{H_{nominal}k}\right)^{\frac{1}{3}}$$
$$where\ \frac{H_0}{H_{nominal}} = 160\,\%\ and\ k = 1.6 \cdot 10^{-4}$$

Three-Way Valves models

$$\dot{m}_{OUT,1} = \dot{m}_{IN}\frac{OF}{100}$$
$$\dot{m}_{OUT,2} = \dot{m}_{IN} - \dot{m}_{OUT,1}$$

2.2 Control strategy

The thermal management system must ensure the proper functioning of the PEM Fuel Cell modules to preserve their useful life. As an increase in electrical load corresponds to a decrease in stack efficiency, a control system must be set up to drain off any excess heat. The goal is to achieve the set point values described in Table 2, suggested by the manufacturer. To do this, three heat exchangers have been provided: two water-water 50%/glycol 50% heat exchangers for the interface between the cooling of the PEM Fuel Cell modules and the MH heating system, and a water-sea water heat exchanger for the dissipation of surplus heat. Three-way flow control valves are installed before the heat exchangers to bypass them and influence the target temperatures directly: cooling outlet temperatures of PEMFCs ($TT11_{A/B}$ and $TT21_{A/B}$) and water-glycol outlet temperatures of WGHEs (TT21 and TT22).

Table 2: temperature set points

Load	$TT11_{A/B}$ and $TT21_{A/B}$ [°C]	TT21 and TT22 [°C]
Idle (50 A)	56	54
Minimum current (120 A)	58	55
Nominal current (400 A)	64	56
Maximum Current (500 A)	65	56

2.3 Case study

This paper presents the case study of the ZEUS, the first certified Italian ship with on-board hydrogen power propulsion, launched in 2022. Two PEM FCS systems (71 kW each) in parallel provide electrical generation to meet both propulsion and hotel loads. The fuel cells are fueled by two MH racks, capacity 50 kg of hydrogen, which are heated using the thermal energy dissipated by the FCS to increase overall system efficiency. A battery system works to fill the energy demand during transients. The main characteristics of the systems described are summarized in Table 3.

Table 3: characteristics of PEMFC and MH system.

PEM Fuel Cells		
Installed modules	2	-
Installed Power (per module)	71	kW
BOP consumption (at 500 A)	11	kW
Stack efficiency (at 500 A)	47	%
Hydrogen storage		
Installed racks	2	-
Hydrogen content per rack	25	kg
Batteries		
Installed modules	84	-
Energy per module	1.84	kWh
Efficiency	96	%

The purpose of the simulations is to verify the robustness of the control strategy systems applied to the MPC method and to make a comparison with a traditional PID control method for safe operations. A ship loading profile is adopted for this purpose, sailing the area between Ischia and Castellammare di Stabia, close to Naples

(Italy). The navigation time is 7 hours with a peak speed of 6 knots, as described in Table 4.

Table 4: load profile of ship energy demand

t [h]	Power [kW]	Profile
0	18.5	Harbor
1	27	Maneuver
1.5	45	Cruise
5.5	27	Maneuver
6	18.5	Harbor
7	18.5	Harbor

The system was initially assumed at equilibrium with an output power of 18.5 kW. The initial state of charge of the metal hydrides is 99%.

3. RESULTS

In this section, the simulation results performed on the thermal management loop of the PEM Fuel Cells and metal hydride system are presented. The applied load profile considers two load steps, from 18.5 kW to 27 kW and then from 27 kW to 45 kW, followed by equal load reductions. The current (model forcing) ramp velocity rate was set at 50 A/s, as suggested by the manufacturer. As shown in the Figure 2, the stacks can produce the required electrical power continuously for the entire duration of the mission. As shown in the figure, the stacks controlled by the MPC method can produce the required electrical power continuously for the entire duration of the mission. During both the load's rise and drop phase, the batteries repetitively deliver and absorb the difference in energy demand-production.

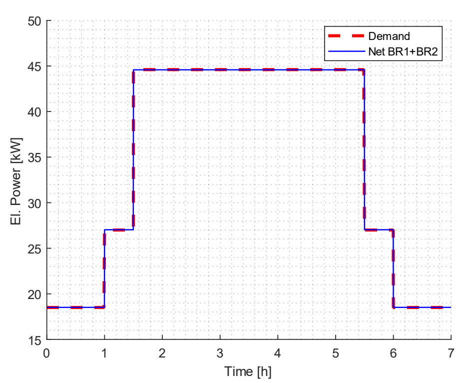

Fig. 2: ship net load power demand and PEM Fuel Cell modules response.

With MPC control system, it is possible to control the cooling temperatures leaving the stacks and the WGHE keeping peaks low and to reduce the time to align with set points. The maximum deviation from the set point is about 1.5 °C and the time required to reach equilibrium is approximately 1 minute, as shown in Figure 3 and Figure 4.

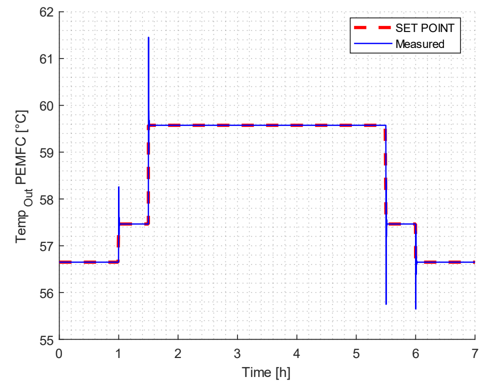

Fig. 3: PEM Fuel Cell cooling outlet temperature against set point.

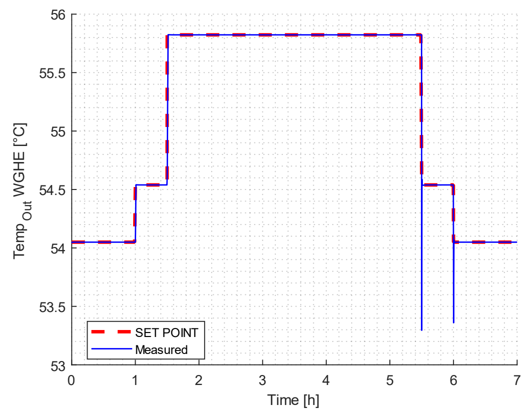

Fig. 4: WGHE water-glycol outlet temperature against set point.

A comparison between the control method with PID and the MPC method is shown in Figure 5 and Figure 6. It is highlighted that the MPC method is the most effective. Both the cooling temperature at the outlet of the fuel cells and the water-glycol temperature at the outlet of the WGHE reach the set point significantly faster than using the PID. It can be observed that during the variation of the electrical load, the cooling outlet temperature of the fuel cells suffers the greatest amplitude variations. It is important to achieve a good stability of this measured value to avoid flooding or drying of the membranes, and the MPC system is much more effective and faster than PID. The set point is approached in a maximum time of 1 min in the MPC case against 3 min in the PID control case.

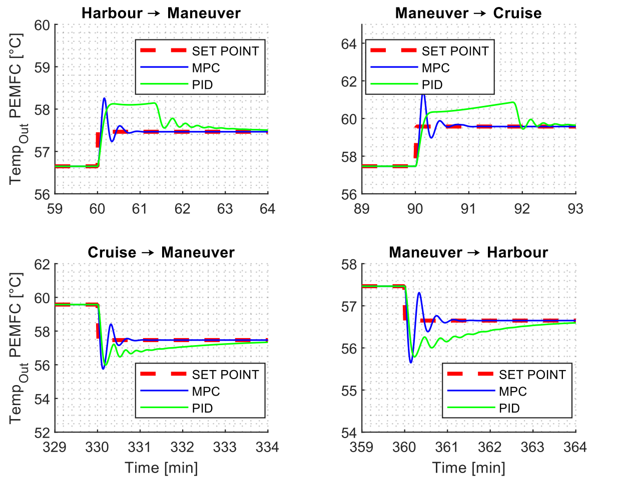

Fig. 5: control comparison between MPC and PID logics for PEM Fuel Cell cooling outlet temperature.

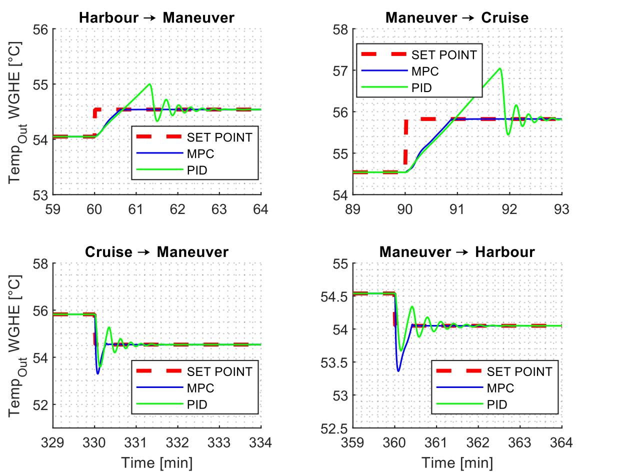

Fig. 6: control comparison between MPC and PID logics for WGHE water glycol cooling outlet temperature.

4. CONCLUSIONS

In this work, the complete dynamic process model of PEM fuel cell system has been developed in the MATLAB-Simulink environment. Simulation results show the comparison between PID and MPC during the transients for a typical load maritime profile, considering the ZEUS hydrogen vessel as test case. The MPC controller guarantees the stability and the fast response of the FC cooling system performance, allowing for transient time lower than 40 seconds. Besides, the MPC avoids the temperature peak in the temperature at WGHE outlet.

The control set-up will be studied more in detail considering different operative conditions, aiming to keep the temperature at optimal level for the FCS+MH thermal management, at the same time preventing conditions that could damage the PEM Fuel Cells.

REFERENCE

[1] www.iea.org/data-and-statistics/ International Energy Agency (IEA) website, access 30/04/2022.
[2] International Maritime Organization (IMO), Fourth Greenhouse Gas Study, 2020, available at www.imo.org
[3] *Maritime forecast to 2050-Energy transition outlook* (2019), DNV-GL Maritime.
[4] J.D. Ampah, A.A. Yusuf, S. Afrane, C. Jin, H. Liu, J. Of Cleaner Production, 2021; 320: 128871.
[5] A. Al-Enazi, E.C. Okonkwo, Y. Bicer, T. Al-Ansari, Energy Reports, 2021; 7: 1962-1985.
[6] C.J. McKinlay, S.R: Turnock, D.A. Hudson, Int J of Hydrogen Energy, 2021; 46: 28282-28297.
[7] O.B. Inal, B. Zincir, C. Deniz, Int J of Hydrogen Energy, 2022.
[8] C. Nuchturee, T. Li, H. Xia, Renew Sustain Energy Rev, 2020; 134: 110145.
[9] N.R. Ammar, I.S. Seddiek, Ocean Engineering, 2020; 215: 107887.
[10]M. Perčić, N. Vladimir, I. Jovanović, M. Koričan, App. Energy, 2022; 309: 118463.
[11]H. Sapra et al., App. Energy, 2021; 281: 115854.
[12]L. Kistner, A. Bensmann, R. Hanke-Rauschenbach, App. Energy, 2022; 316: 119052.
[13]M. Ye, P. Sharp, N. Brandon, A. Kucernak, , Int J of Hydrogen Energy, 2022; 47: 8565-8584.
[14]L. van Biert, M.Godjevac, K.Visser, P.V.Aravind, J. of Power Sources, 2016; 327: 345-364.
[15]O.B. Inal, C. Deniz, , J. of Cleaner Production, 2020; 265: 121734.
[16]M. Rivarolo, D. Rattazzi, T. Lamberti, L. Magistri, Int J of Hydrogen Energy, 2020; 45: 25747-25757.
[17]E. Gadducci, T. Lamberti, D. Bellotti, L. Magistri, A.F. Massardo, 2021, Int J of Hydrogen Energy, 2021; 46: 24503-24317.
[18]A.M. Bassam, A.B. Phillips, S.R: Turnock, P.A. Wilson, Int. J. of Hydrogen Energy, 2017; 42: 623-635.
[19]L.E. Klebanoff, et al., Int. J. of Hydrogen Energy, 2021; 46: 38051-38072.
[20]Y. Tang, W. Yuan, M. Pan, Z. Wan, App. Energy, 2011; 88: 68-78.
[21]A. Giugno, L. Mantelli, A. Cuneo, A. Traverso, Applied Energy, 2020; 279: 115785.
[22]A. Bouakkaz, A.J.G. Mena, S. Haddad, M.L. Ferrari, J of Energy Storage, 2021: 33; 101887.
[23]K. Darowicki, E. Janicka, M. Mielniczek, A. Zielinski, L. Gawel, J. Mitzel, J. Hunger, App. Energy, 2019; 251: 113396.
[24]X. Li, K. Han, Y. Song, Int. J. of Hydrogen Energy, 2020; 39: 20312-20320.
[25]R. Moradi, K.M. Groth, Int. J. of Hydrogen Energy, 2019; 44: 12254-12269.

[26]M.V. Lototskyy, I. Tolj, L. Pickering, C. Sita, F. Barbir, V. Yartys, Progress in Natural Science: Materials International, 2017; 27: 3-20.
[27]H.Q. Nguyen, B. Shabani, Int J of Hydrogen Energy, 2021; 46: 7738-7745.
[28]D. Chabane, M. Ibrahim, F. Harel, A. Djerdir, D. Candusso, O. Elkedim, , Int J of Hydrogen Energy, 2019; 44: 27553-27563.
[29]M. Cavo, E. Gadducci, D. Rattazzi, M. Rivarolo, L. Magistri, Int. J. of Hydrogen Energy, 2021; 46: 32630-32644.
[30]G. Han et al., App Energy, 2020; 259: 114175.
[31]L. Wang, P.C. Young, J. Process Control, 2006; 16: 355–371.
[32]Y. Wang, H. Li, H. Feng, H. Han, S. He, M. Gao, En. Conv. And Management, 2021; 249: 114851.